Ultrasound in Med. & Biol. Vol. 15, No. 1, pp. 67–72, 1989
Printed in the U.S.A.

0301-5629/89 $3.00 + .00

●*Original Contribution*

AN EXPLANATION FOR THE DECREASE IN CELL LYSIS IN A ROTATING TUBE WITH INCREASING ULTRASOUND INTENSITY

MORTON W. MILLER, CHARLES C. CHURCH, ANDREW A. BRAYMAN, MICHELLE S. MALCUIT† and ROBERT W. BOYD†
Department of Biophysics, School of Medicine and Dentistry, †Institute of Optics, The University of Rochester, Rochester, NY 14642, 14627†

(*Received* 7 *April* 1988; *in final form* 21 *June* 1988)

Abstract—Previous observations indicate that for *in vitro* mammalian cells insonated in a rotating test tube the amount of cell lysis initially increases to some maximum and then decreases with further increase in ultrasound exposure. The results of the present investigation support the postulate that the reduction in cell lysis with increase in ultrasound intensity is related to the development of an ultrasonically induced "cloud" of bubbles in the fluid between the transducer and test tube; these bubbles mitigate against acoustic transmission thus reducing cell lysis in the insonated test tube.

Key Words: **Cell lysis, Gas bubbles, Acoustic cavitation, Rotating test tube.**

INTRODUCTION

A number of investigators have reported that under specific exposure conditions, ultrasound-induced cell lysis is biphasic with respect to ultrasound intensity. For cells contained in a rotating tube positioned in an aqueous water bath, and with the ultrasound beam perpendicular to the side of the test tube, the amount of cell lysis initially increases with increasing ultrasound intensity, reaches some maximum, and then decreases with further increases in ultrasound intensity (Clarke and Hill, 1970; Fu et al., 1980; Kaufman et al., 1977; Kaufman, 1985). Figure 1 depicts the generality of this observation. A similar observation has been made for *in vitro* cells insonated while in acoustically transparent (teflon) "baggies" (Kaufman and Miller, 1978).

The purpose of the present investigation was to gain insight into a physical mechanism of action which would explain the results described above. The results of several investigations have supported the postulate that acoustic cavitation is the dominant mechanism causing cell rupture in *in vitro* cell exposure systems (NCRP Report, 1983; Ciaravino et al., 1981; Sacks et al., 1982). Moreover, a standing wave field is known to arise within the unmodified plastic test tube cell exposure system under the condition of continuous wave insonation (Kaufman and Miller, 1978; Church et al., 1982). One would intuitively expect that as free field intensity increases, the degree and amount of acoustic cavitation occurring in the rotating tube would increase proportionally, producing a concomitant increase in cell lysis. This expectation is met only at low exposure levels (*i.e.*, $< \sim 10 W \cdot cm^{-2}$). At higher intensities the frequency of cell rupture decreases with increasing ultrasound intensity. The uniformity of the results among investigators using differing insonation systems suggests that the operative mechanism responsible for the diminution of cell lysis at ultrasound intensities above a certain level is related to conditions outside the cell container which result in reduced cell exposure and thus reduced cell lysis.

The postulate which guided the present research was that a cloud of bubbles is developed in the aqueous medium between the exposure tube and the transducer which at certain bubble volume densities mitigates against acoustic transmission. This postulate was tested in three ways: (1) observation and measurement of the amount of acoustic cavitation in both the area between the tube and the transducer and in the rotating test tube; (2) comparison of the extent of ultrasound-induced cell lysis with the number of visible bubbles in the fluid between the transducer and test tube at various ultrasound intensities; and (3) placement of "screens" of variously sized bubbles in that area and measurement of acoustic transmission.

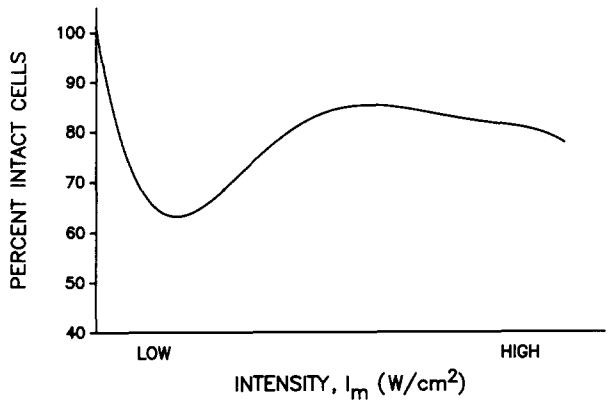

Fig. 1. Generalized pattern for percent intact cells vs. relative ultrasound intensity for *in vitro* cells insonated in a rotating test tube.

MATERIALS AND METHODS

Cell lysis experiments

It was considered important to verify the biphasic dose response curve outlined above. Two replicate experiments were conducted. For each experiment monolayer Chinese hamster ovary (CHO) cultures were established approximately 48 h before use. Cells were grown in F10 medium supplemented with 10% (v:v) fetal bovine serum (FBS). The cells were in log phase growth when harvested; the apparent generation times of the cultures used in Experiments 1 and 2 were 16.0 and 14.7 h, respectively.

Cells were harvested by trypsinization and were diluted with additional F10/FBS to a final volume density of 1×10^5 cells $\cdot$ cm^{-3}. A 4 ml aliquot of this suspension was pipetted into each of 10 screw-cap polystyrene tubes per experiment. The cell suspensions were maintained in a 37°C waterbath until experimental use. The tubes containing the suspension were swirled at approximately 2-min intervals to maintain the cells in suspension.

Immediately prior to the 1-min ultrasound/sham exposure, a 1.0 ml aliquot of cell suspension was removed from the suspension to be exposed. This aliquot was diluted 1:9 with physiological saline, and the cell concentration determined using a Coulter counter. The remaining 3 ml of suspension were then exposed/sham exposed to 1 MHz ultrasound of defined intensity for 1 min (Fig. 2). The exposure system was the same as used by Kaufman and Miller (1978; *vide* their Fig. 4); the test tube was 7.3 cm from the transducer. After treatment, a second 1 ml aliquot was removed from the suspension for Coulter counting as described. The entire process was repeated for each tube. Ultrasound intensity was based on a steel ball radiometric calibration at 1 W/cm^2 with an assumption of linear increase to 35 W/cm^2. No bubbles were observed in the fluid at 1 W/cm^2, and changes to higher dB settings were made quickly. Thus bubbles do not affect the impedance of the exposure system while setting to higher intensity values. Ultrasound intensities (I_m *vide* NCRP, p. 59) used were: 0, 1, 5, 10, 15, 20, 25, 30, and 35 W/cm^2; the exposures took place in ascending order, except that a 0 W/cm^2 sham treatment was also included after the 35 W/cm^2 treatment as a control against culture "aging" during the course of the experiment. The culture age (in minutes, after trypsinization; *i.e.*, time spent in suspension) was recorded at the onset of each exposure treatment. These data allowed assessment of apparent cell lysis due to cell attachment to the polystyrene tubes. The duration of each experiment was approximately 45 min. Experimental data were expressed as the percentage of intact cells per ml (PIC) present in the cell suspension after insonation, relative to the number of intact cells immediately before treatment.

One additional cell lysis experiment was undertaken. A Hartman® fish tank aerator stone, powered by a Hartman® fish tank airpump, was placed at the bottom of the ultrasound exposure tank such that a stream of bubbles flowed upward between the transducer and the rotating test tube containing the cells (Fig. 3). No bubbles were observed to attach to the rotating test tube. Lysis was determined for 1 min exposures to ultrasound at intensities ranging from 0–35 W/cm^2 (open circles, as was done for Fig. 2) but also included a series of exposures involving insonation through a continuous array of bubbles produced by the Hartman® fish tank aerator stone.

Photon detection

A photon counting system was used to detect transient cavitational events in the insonated de-

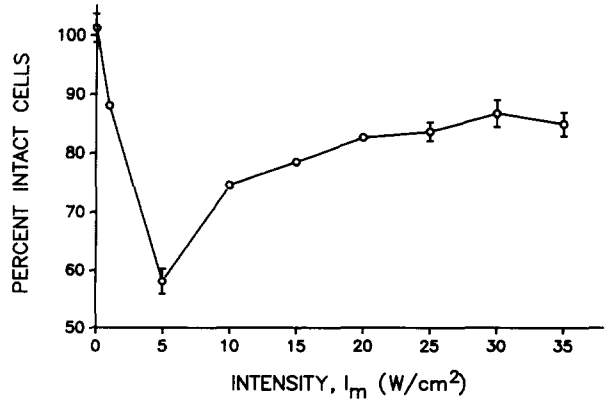

Fig. 2. Percent intact cells vs. 1 MHz ultrasound intensity 0–35 W/cm^2. Mean ± standard error.

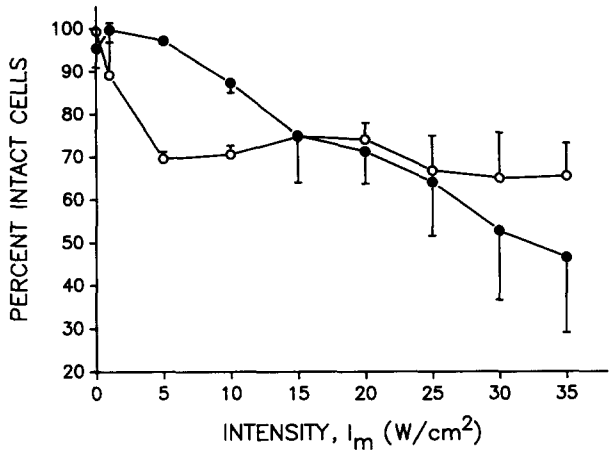

Fig. 3. Percent intact cells vs. 1-MHz ultrasound intensity; (open circles) = horizontal exposure; (solid circles) = horizontal exposure plus Hartman® fish tank aerator-generated bubbles. Mean ± standard error.

gassed water between the test tube and the transducer and within the test tube itself. The rationale for the use of photon detection was that the number of transient events is quantified reasonably well by counting the number of photons produced in a sonicated liquid, even though the precise relationship between numbers of photons and numbers of bubbles is not known. We had observed our insonation procedure under dark-adapted conditions and noted the faint emission of light at higher ultrasound intensities (10–30 W/cm^2).

The detection apparatus consisted of a fast photomultiplier tube (PMT) and a photon counter. The light was detected by a Thorn EMI photomultiplier tube (model 9863Q) that was cooled to −30°C to keep the dark count at ≤20 counts/s. The photo events were analyzed by a Stanford Research SR400 gated photon counter with discriminator. The experiment entailed measuring the light intensity as a function of the ultrasound intensity. All photon detection regimens lasted 30 s each.

For photon detection in the area between the transducer and test tube the PMT was positioned outside the water tank between the transducer and test tube at a distance of about 10 cm from the interaction region; the apenture of the photon detector had a diameter of 1 cm. Any photon emitted in the bathing solution in the tank and at an angle to intersect the photon detector aperture would be detected. For photon detection within the test tube the PMT was placed about 2 cm above the top of the test tube; the internal diameter of the test tube was 1.2 cm. The top surface of the tank was covered with thick cardboard and black electrician's tape, and the outer surface of the test tube had received a thick coat of black enamel paint; these steps were taken to insure that the measured light originated from within the test tube.

To enhance the emission of photons inside the test tube a 10^{-4} M solution of Luminol (Eastman Kodak, 3606) was used. Luminol was dissolved in 0.1 M KOH-boric acid buffer, made 10^{-7} M in C_0(II)Cl, and pH adjusted to 10.9 (Burdo and Seitz, 1975). The Luminol solution (3 ml) was placed in the test tube, and the exposure tank was filled with degassed water.

Bubble-mediated mitigation of ultrasound field propagation

Two types of special-order hydrophobic Nucleopore Corporation membranes were used: membrane 51A5D, with a manufacturer's reported pore diameter of 2.9 micrometers and a density of 0.86×10^5 pores · cm^{-2}, and 51A5E with a reported pore diameter and pore density of 4.6 micrometers and $0.76 \times 10^5 \cdot \text{cm}^{-2}$, respectively. Ten-centimeter diameter metal rings were constructed from steel wire (diam ≃ 2 mm). A portion of one membrane was then cut to overlay the round metal frame, to which it was cemented with Goodyear RTV® rubber sealant.

The diameters of 100 pores in each type of membrane were measured to verify manufacturer's data. A calibrated ocular micrometer in a Zeiss microscope (100× objective, 10× ocular, 1.25× optivar) was used to measure two diameters (horizontal, vertical) of each pore; an average diameter per pore was then calculated. The number of pores per microscope field was also determined as was the area per microscope field. The total bubble intercept area was calculated using the average bubble area multiplied by the bubble area density divided by the total membrane area.

Metal rings with attached membranes were placed individually into the exposure tank, and positioned such that the ultrasound beam passed through the central area of the ringed membrane. The intensity of the sound field at the position of the exposure tube, ~7.3 cm from the transducer, was determined from the deflection of a small steel ball with or without the membrane in place. A low intensity (1 W/cm^2) continuous wave ultrasound exposure was used. The general procedure was to ascertain the amount of deflection of the steel ball without the membrane in place, turn the sound field "off," insert the ringed membrane at about 3 cm from the transducer, re-energize the transducer to the same output and remeasure the amount of deflection of the steel ball, taking several measures from as quickly as possible, to 3 min. Some metal frames with membranes were autoclaved in water (1 atm, 115°C) to remove

gas and were then used in transmission determinations. The deflection of the steel ball was also determined with and without bubbling from the Hartman® aeration stone at 1 W/cm^2.

Visible bubble counts

The numbers of visible bubbles in the water between the test tube and the horizontal transducer over the intensity range 0–35 W/cm^2 were determined from visual counts of bubbles from 20 × 25 in photographs (enlargement magnification ~ 1.7). Kodak Technical Pan 35 mm film was used to photograph the cell exposure apparatus. An electronic flash was used for illumination. The direction of the flash was from behind the tank to provide a dark field effect. After exposure the film was developed in Duraflow® in a Versamat Model 5 processor at 3.6 cm/s. Prints were made on Polycontrast Rapid II RC photographic paper. An Agfa Lupe 8× standing image magnifier was used to count the bubbles in the fluid in the area between the insonated test tube (miniscus of fluid within tube to tube bottom) and the transducer. All prints were scored blindly.

RESULTS

Analysis of pre-exposure cell counts as a function of time post-trypsinization showed no significant change in cell concentration over the course of the experiments ($p > 0.2$; data not shown). Thus, despite the fact that the cells were maintained at 37°C rather than on ice, cell attachment to the polystyrene tubes was negligible.

In experiments in which no exogenous bubbles are placed between transducer and cells, cell concentration was markedly affected by 1-MHz ultrasound treatment (Fig. 2). CHO cell PIC declined rapidly with increasing intensity from 0–5 W/cm^2; the minimum PIC observed occurred at 5 W/cm^2, and represented about 40% cell lysis (58% PIC). With increasing ultrasound intensity, PIC increased, most rapidly over the interval of 5–10 W/cm^2, and more slowly but consistently with further increases in intensity. A relatively constant PIC of about 85% was attained at intensities ≥20 W/cm^2.

A second series of experiments involved the insertion of a filter membrane with either gas-filled or degassed, micron-range pores between the transducer and the cells. Prior to the conduct of these experiments, it was considered important to quantify the actual pore sizes and area densities of the two membrane types used. Nucleopore Corporation data sheets indicated pore diameters of 4.6 and 2.9 μm for 51A5E and 51A5D, respectively; our data indicated average pore diameters of 5.6 and 3.1 μm, respectively (Table 1). From our own determinations of the average bubble sizes, numbers and surface area densities, the percent total bubble cross-sectional area was calculated to be 2.2 and 0.5% for the 51A5E and 51A5D membranes, respectively (Table 1).

The relative transmissibility of ultrasound through non-autoclaved and autoclaved hydrophobic membranes is shown in Table 2; the percent deflection is approximately equal to intensity in W/cm^2. Membrane 51A5D has an approximate twofold higher transmissibility than membrane 51A5E. For both membranes, the initial measured transmissibility values were lower than those obtained at later times. For autoclaved membranes the presence or absence of the membrane could not be distinguished by use of the radiometer: in both cases, ultrasound transmission was 100%. When the Hartman® aerator

Table 1. Pore diameter and total pore intercept area for nucleopore hydrophobic membranes 51A5D and 51A5E.

Parameter	Nucleopore membrane	
	51A5E	51A5D
Investigator's Measurements		
Pore diameter (μm)†	5.6 ± 0.4 (S.D.)	3.1 ± 0.8 (S.D.)
(df)	(94)	(99)
Average pore area/pore (μm^2)	24.6	7.5
No. pores/microscope field	18 ± 4.1 (S.D.)	12.4 ± 3.6 (S.D.)
(df)	(29)	(29)
Pores/cm^2	0.88×10^5	0.86 ± 10^5
Total cross-sectional pore area/microscope field (2 × 3) (μm^2)	442.8	93.6
Microscope field diameter (μm)	161 ± 1.5	161 ± 1.5
Microscope field area (μm^2)	20,358	20,358
Percent pore cross-sectional area to microscope field area (4 ÷ 6)	2.2	0.5
Manufacturer's Data		
Pore diameter (μm)	4.6	2.9
Pores/cm^2	0.76×10^5	0.86×10^5

† Using a Zeiss Photomicroscope: 100× objective, 10× ocular, 1.25 optivar.

Table 2. Percent deflection† with time of a steel ball radiometer with an interspersed, unautoclaved‡ hydrophobic membrane.

Nucleopore membrane	Descriptive statistic	Time Lapse from field onset (s) Immediate	20	40	60	120	180
	X	36	46	49	51	55	54
51A5E	SD	5	5	3	3	3	2
	n	5	5	5	5	5	5
	X	76	88	93	94	95	96
51A5D	SD	2	2	1	1	1	1
	n	5	5	5	5	5	5

† Relative to deflection without membranes present.
‡ For autoclaved membranes at all intervals, transmission was 100%.

was used to produce a large bubble screen, there was no measurable deflection of the radiometer; transmissibility was essentially zero when the calculated output was 1 W/cm^2.

Cell lysis data reveal that there is an initial drop in the percent intact cells with initial increase in ultrasound exposure from 1 to 5 W/cm^2 (Fig. 3); the results are generally consistent with those previously obtained in that cell lysis is less at the higher exposure intensities (Fig. 2). When bubbles from a Hartman® aerator are imposed between the test tube and transducer, there is a dramatic decrease in cell lysis at 5 W/cm^2, and a general linear decrease in percent intact cells with increase in ultrasound intensity to the maximum output capability of the system (35 W/cm^2; Fig. 3). As I_m rises some energy does get through the system, thus cells are lysed.

The number of visible bubbles in the water between the insonated test tube and the transducer correlated with ultrasound exposure intensity (Table 3); there was a dramatic rise in bubble counts in the 5–10 W/cm^2 exposure range, with an approximate eightfold increase in bubble counts with a doubling of ultrasound intensity.

The number of photons per second emitted from the region between the transducer and the test tube increased dramatically as the ultrasound intensity was increased above 10 W/cm^2 (Fig. 4). The number of photons per second from the insonated test tube increased dramatically from 5–10 W/cm^2, then underwent a modest decline in the 15–25 W/cm^2 intensity range and subsequently reached a second high count at 35 W/cm^2 (Fig. 5).

Table 3. Number of visible bubbles per photograph using degassed water between rotating exposure tube and transducer in exposure tank.

Ultrasound intensity (W·cm^{-2})	Trial 1	Trial 2	Ave.
0	33	63	48
1	58	67	63
5	26	47	37
10	197	355	276
15	306	238	272
20	359	466	413
30	746	647	697

DISCUSSION

The collective data support the postulate that as a cloud of ultrasonically generated bubbles collects in the area between the transducer and polystyrene test tube, cell lysis diminishes. First, it is clear that cell lysis is at a maximum (for this particular cell exposure system) at an intensity of about 5 W/cm^2. Above this level, lysis diminishes with an increase in ultrasound intensity. When bubbles from a fish tank aera-

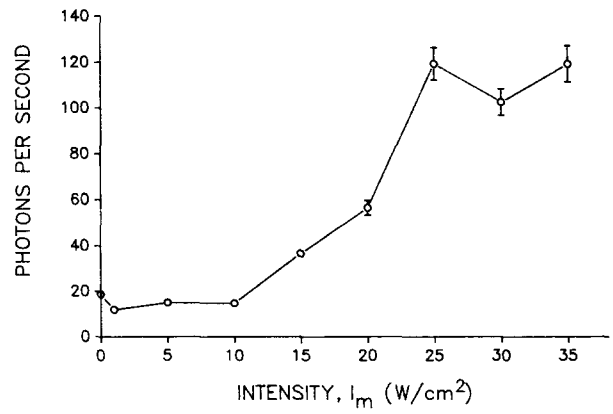

Fig. 4. Photon counts per second in area between transducer and rotating (~30 rpm), test tube vs. approximate† ultrasound intensity (0–35 W/cm^2). Error bars = S.E.M. †The descriptor "approximate" denotes that the exposure system was calibrated (steel ball radiometer deflection) in one building and then used in another building for photon detection. It was not feasible to undertake calibration under photon detection conditions.

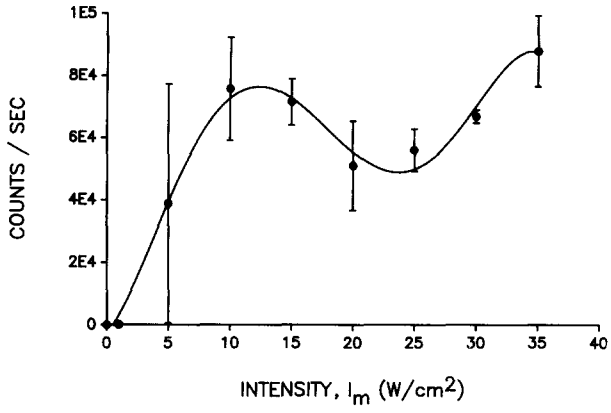

Fig. 5. Photon counts per second from rotating (~30 rpm) test tube vs. approximate† ultrasound intensity (see Fig. 4 legend for elaboration on ultrasound intensity calibration).

tor were imposed between the test tube and transducer there was a dramatic decrease in cell lysis at 5 W/cm^2, and a general linear decrease in percent intact cells with increase in ultrasound intensity to the system's maximum output. There is no significant increase in visible bubble count for the transducer-test tube area (TTA) at 5 W/cm^2 or less. Above 5 W/cm^2 the number of TTA bubbles dramatically increases with an increase in ultrasound intensity; above 10 W/cm^2 the numbers of photons per second likewise increases with increase in ultrasound intensity. Within the insonated test tube photon emission was maximal at about 10 W/cm^2. We consider these two observations (maximum cell lysis at 5 W/cm^2, maximum photon emission at about 10 W/cm^2) as being internally consistent; since the test tube remains in the system while ultrasound intensity is changed, the acoustic impedance will vary. Thus, there is error in intensity that is especially significant near threshold. Thus, we conclude that the cloud of TTA bubbles generated at high ultrasound intensities mitigates against ultrasound transmission to the test tube, with concomitant reduction in cell lysis.

That bubbles mitigate against ultrasound transmission is well known, and is both qualitatively and quantitatively demonstrated in the present study. Bubbles of radii much larger than the linear resonance radius at the frequency of interest will remove energy from a sound field primarily by scattering, with scattering cross sections approximately equal to their geometrical cross sections. Smaller bubbles both scatter and absorb energy from the field, with absorption predominating as the resonance radius is approached. In fact the absorption cross section of a resonant bubble may be several orders of magnitude greater than the geometrical cross section, although it must be remembered that resonant bubbles will not be trapped in a standing wave field and therefore probably do not contribute greatly to the effects investigated here.

At high ultrasound intensities (*e.g.*, 30–35 W/cm^2) there is a large amount of photon emission (Fig. 5) but relatively less cell lysis (Fig. 2). These results will appear inconsistent if it is assumed that all pressure antinodes are occupied by the same number of bubbles at all times and that all transient events, regardless of severity, produce the same number of photons. Such assumptions would allow one to infer a constant relationship between number of photons counted and number of cells lysed. Although plausible, neither assumption is justified on the basis of experimental evidence. Thus the lack of a one-to-one correspondence between the tails of Figs. 2 and 5 is not of great concern.

Acknowledgement—This research was supported by US PHS CA39230. The authors thank Mr. Yige Chen for excellent technical assistance.

REFERENCES

Biological effects of ultrasound: Mechanisms and clinical implications. National Council on Radiation Protection and Measurement (NCRP), Report No. 74, Bethesda, MD. (USA) 20814; 1983:146–149.

Burdo, T. G.; Seitz, W. R. Mechanism of cobalt catalysis of luminol chemiluminescence. Anal. Chem. 47:1639–1643; 1975.

Church, C. C.; Flynn, H. G.; Miller, M. W.; Sacks, P. G. The exposure vessel as a factor in ultrasonically-induced mammalian cell lysis—II. An explanation of the need to rotate exposure tubes. Ultrasound in Med. & Biol. 8:299–309; 1982.

Ciaravino, V.; Miller, M. W.; Carstensen, E. L. Pressure-mediated reduction of ultrasonically induced cell lysis. Rad. Res. 88:209–213; 1981.

Clarke, P. R.; Hill, C. R. Physical and chemical aspects of ultrasonic disruption of cells. J. Acoust. Soc. Am. 50:649–653; 1970.

Fu, Y-K.; Miller, M. W.; Lange, C. S.; Griffiths, T. D. Ultrasound lethality to synderonous and asynderonous Chinese hamster V-79 cells. Ultrasound in Med. & Biol. 6:39–46; 1980.

Kaufman, G. E. Mutagenicity of ultrasound in cultured mammalian cells. Ultrasound in Med. & Biol. 3:497–501; 1985.

Kaufman, G. E.; Miller, M. W. Growth retardation in Chinese hamster V-79 cells exposed to 1 MHz ultrasound. Ultrasound in Med. & Biol. 9:139–144; 1978.

Kaufman, G. E.; Miller, M. W.; Griffiths, T. D.; Ciaravino, V. Lysis and viability of cultured mammalian cells exposed to 1 MHz ultrasound. Ultrasound in Med. & Biol. 3:21–25; 1977.

Sacks, P. G.; Miller, M. W.; Church, C. C. The exposure vessel as a factor in ultrasonically-induced mammalian cell lysis. I. A comparison of tube and chamber systems. Ultrasound in Med. & Biol. 8:289–298; 1982.